Scene Inference for Object Illumination Editing

Zhongyun Bao[1], Chengjiang Long[2]*, Gang Fu[1], Daquan Liu[1], Yuanzhen Li[1], Jiaming Wu[1], Chunxia Xiao[1,3,4]*
[1]School of Computer Science, Wuhan University, Wuhan, Hubei, China
[2] JD Finance America Corporation, Mountain View, CA, USA
[3]National Engineering Research Center For Multimedia Software, Wuhan University, Wuhan, Hubei, China
[4]Institute of Artificial Intelligence, Wuhan University, Wuhan, Hubei, China
cjfykx@gmail.com, xyzgfu@gmail.com, {zhongyunbao, cxxiao}@whu.edu.cn

Abstract

The seamless illumination integration between a foreground object and a background scene is an important but challenging task in computer vision and augmented reality community. However, to our knowledge, there is no publicly available high-quality dataset that meets the illumination seamless integration task, which greatly hinders the development of this research direction. To this end, we apply a physically-based rendering method to create a large-scale, high-quality dataset, named IH dataset, which provides rich illumination information for seamless illumination integration task. In addition, we propose a deep learning-based SI-GAN method, a multi-task collaborative network, which makes full use of the multi-scale attention mechanism and adversarial learning strategy to directly infer mapping relationship between the inserted foreground object and corresponding background environment, and edit object illumination according to the proposed illumination exchange mechanism in parallel network. By this means, we can achieve the seamless illumination integration without explicit estimation of 3D geometric information. Comprehensive experiments on both our dataset and real-world images collected from the Internet show that our proposed SI-GAN provides a practical and effective solution for image-based object illumination editing, and validate the superiority of our method against state-of-the-art methods.

1. Introduction

The task of image composition is to integrate an object with the real-world scene to generate a synthesized image with harmonious illumination. However, as the illumination of objects is usually inconsistent with the scene, the quality of synthesized image would be significantly downgraded. Although the existing retouching software, such as photoshop, is relatively mature, it is difficult for an experienced retoucher to make an ideal synthesized image with illumination harmonization. Especially for object shadow generation in the scene, it requires precise matting skills, a slight flaw will lead to very poor result. To this end, we propose a SI-GAN for user-friendly automatic illumination editing, even an inexperienced user can easily complete object illumination editing, and achieve realistic and harmonious illumination for the inserted object.

(a) (b) (c) (d)

Figure 1. Illumination editing for an inserted object in a single image. (a) 2D foreground object. (b) Background image. (c) Naive composite image. (d) Illumination harmonized image.

Automatically editing illumination for inserted object to achieve scene illumination harmonization is a challenging operation in computer vision and AR applications. Karsch et al. [17] presented an image editing system that supports drag-and-drop 3D object insertion, and Liao et al. [23, 24] proposed an approximate shading model for image-based object modeling and insertion. Although these methods produce perceptually convincing results, their performances highly depend on the quality of the estimated geometry, shading, albedo and material properties. However, in some cases, any errors or inaccurate estimation in either geometry, illumination, or materials may result in unappealing editing effects. Different from these methods, in this work, we aim to explore a deep learning-based method to directly learn mapping relationship between the inserted object illumination and the real-world scene, and achieve scene illumination harmonization without any explicit inverse rendering (recovering 3D geometry, illumination, albedo and material).

As deep learning-based method calls for a large num-

*This work was co-supervised by Chengjiang Long and Chunxia Xiao.

ber of data. Especially in this task, a dataset with a lot of training image pairs of synthesized images without illumination harmonization and corresponding ground truth with illumination harmonization is desired. Existing dataset like iHarmony4 [3] by generates synthesized images based on COCO, contains pairs of synthesized image and corresponding harmonized image, but all these synthesized images lack shadow for inserted object. It does not provide sufficient shadows and illumination information for augmented reality applications. Although shadow-AR dataset [25] with inserted object shadow information is conducive to our task by providing sufficient shadow clues of object and scene, it does not take into account the shading information of the inserted object.

In this work, we construct a first large-scale, high-quality synthesis image dataset named IH dataset for the object relighting task. Our dataset contains 89,898 six-tuples, each with one input triplet (*i.e.*, a naive composite image, and the corresponding object mask and background mask), and another ground truth triplet (*i.e.*, an object illumination map, a background illumination map, and a final illumination harmonization image). See Figure 2 for a six-tuples example. To build our dataset, we collect many HDR images from Laval's HDR dataset [7, 6] and HDR panoramas from the Internet taken in various indoor and outdoor real-world scenes. Therefore, the scenes in our dataset are general and challenging. In addition, we also collect 7 3D object models with considerably different shapes and postures.

To produce harmonized illumination for the inserted object, inspired by spatial attention learning [40, 12, 36, 35, 13, 10, 30] and adversarial learning [8, 1], we propose a novel learning-based scene inference algorithm named SI-GAN. SI-GAN takes a naive composite image with shadow-free object as well as inserted object mask as input, and makes full use of multi-scale attention mechanisms and adversarial learning to directly infer mapping relationship between the inserted foreground object and corresponding background environment.SI-GAN edits object illumination according to the proposed illumination exchange mechanism in parallel network, and can directly generate plausible the object shadows, illumination to make the image more harmonious and realistic. Compared with the previous methods [17, 23, 24], our work avoids explicit inverse rendering, e.g. complicated geometry, illumination and reflectance estimation, and directly achieves high-quality harmonized object illumination editing results. A visual example is shown in Figure 1. Our main contributions are summarized as follows:

- We construct the first large-scale, high-quality image illumination harmonization dataset IH, which consists of 89,898 image six-tuples with a diversity of real-world background scenes and 3D object models.
- We propose a novel deep learning-based scene inference algorithm named SI-GAN, a multi-task collaborative network, which can directly perform illumination harmonization editing for the inserted object without explicit inverse rendering.
- Extensive experiments show that the proposed SI-GAN can effectively achieve high-quality image illumination harmonization and significantly outperforms existing state-of-the-art methods.

2. Related work

In this section, we briefly review the related work on object illumination editing, shadow generation, image-to-image translation, respectively.

Object illumination editing. Traditional object illumination editing methods mainly concentrated on estimating the scene geometry, illumination and surface reflectance to edit the object. Previous methods [19, 16] have shown that coarse estimates of scene geometry, reflectance properties, illumination, and camera parameters work well for many image editing tasks. These methods require a user to model the scene geometry and illumination. The method [2] not only recovers shape, surface albedo and illumination for entire scenes, but also requires a coarse input depth map, while this method is not directly suitable for illuminating inserted object. Similar to these methods, Karsch et al. [17] presented a fully automatic method for recovering a comprehensive 3D scene model (geometry, illumination, diffuse albedo and camera parameters) from a single low dynamic range photograph. Liao *et al.* [24] presented an object relighting system that supports image-based relighting, although this method achieves impressive result, it still needs to reshape the object and model the scene.

These methods depend on the physical modeling of object and scene information, and inaccurate reconstruction results will lead to poor results. In contrast, our method automatically edits the object illumination, directly generates the harmonized illumination results without complicated inverse rendering, and thus produces better visual effects.

Shadow generation. Recently, with the breakthrough in adversarial learning, generative adversarial network(GAN) [8, 1, 27] have been successfully applied to shadow detection, removal and generation [31, 32, 5, 38, 11, 39, 37, 25]. For shadow generation, Liu *et al.* [25] proposed an ARShadowGAN model, which is able to directly model the mapping relation between the shadow of the virtual object and the corresponding real-world environment based on their constructed dataset. Similar to this method, our method also aims to generate the object shadow without explicit estimation of 3D geometric information. Besides that, our method considers the shading of the object itself. We not only realize reasonable object shadow generation

(a) (b) (c) (d) (e) (f) (g) (h) (i) (j)

Figure 2. The illustration of a synthesized illumination harmonization image generation process. Given a 3D object (a), we first apply a panorama illumination (b) to render the 3D object and get an image-based object(d). Then we paste the image-based object into a background image (e) directly without any illumination adjustment. In this way, along with an object mask (g) and a background mask (h), we get an image (f) with illumination and shadow inconsistency between object and its surrounding. With the background illumination map (c), we then use Blender to synthesize the illumination harmonization image (i) and take it as the ground-truth for supervised learning. (j) is zoomed-in local details marked in (i). Note we consider (f), (g) and (h) as an input triplet, and (b), (c) and (i) as a ground truth triplet. An input triplet and corresponding ground truth triplet are treated as a six-tuple in our dataset. *Better view in electronic version.*

with the same effect as Liu *et al.*'s algorithm, but also edit the object illumination to achieve overall scene illumination harmonization.

Image-to-image translation. Image-to-Image translation is to map an input image to a corresponding output image. It has been widely used in various tasks, including super-resolution[18, 21], image quality restoration [26, 33], image harmonization [14, 3], and so on. It is worth mentioning that Cong et al. [3] proposed a novel domain verification discriminator, with the insight that the foreground needs to be translated to the same domain as the background for image harmonization. But they focus on the illumination of foreground object and do not consider object shadow generation task. Different from this work, our task takes into account both illuminating the object and generating the shadow of the object, and achieves illumination harmonization for the whole scene.

3. Our IH Dataset

3.1. Dataset building

The construction process of our IH dataset includes four steps: collecting images, filtering images, and rendering as well as compositing. In the following, we will describe these steps in detail.

Collecting images. We first choose all images from the Laval's HDR dataset [7, 6], and collect 2,686 HDR panorama images from the Internet with a diversity of real-world scenes. For each panorama map, we extract 8 limited field-of-view crops to produce the background images, and also use it as illumination to render ground truth results. We initially obtain 22,256 background images in total. Also, we collect 60 3D models as inserted objects, such as *bunny* and *lucy*.

Filtering images. To ensure the quality of the dataset for our object relighting task, we further filter out the following three kinds of images: (i) without obvious or natural-looking illumination, (ii) without a reasonable place to insert virtual object, and (iii) with inconspicuous or no shadows. In this way, we finally obtain 12,253 remaining background images.

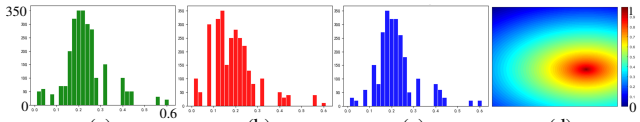

(a) (b) (c) (d)

Figure 3. Statistics on the ratio of (a) virtual objects, (b) real object, (c) real shadow, and (d) illumination. Note that x and y axes in (a)-(c) have the same scale and meaning (*i.e.*, x: ratio; y: count).

Rendering and compositing. With collected 3D models, background images, and the corresponding panorama maps, the ground truth object relighting images (see Figure 2 (i)) are rendered using Blender. We first specify a plane at the bottom of the inserted object for casting shadows, then embed the 3D object into the cropped background image, and finally use the corresponding environment map to render the illumination of the object to produce the final result. Note that we use Photoshop to manually annotate each object in our dataset to produce their mask images.

We use 60 virtual models with different pose configures using the pipeline shown in Figure 2 to construct our dataset based on different background images and produce 169,672 synthesized ground truth illumination harmonization images in total. Finally, to improve training efficiency, we only use 89,898 six-tuples to train the our network. Each six-tuple consists of two triplets. One triplet as input data includes a synthetic image without any illumination adjustment, and the corresponding object mask and background mask. The other one as ground-truth data includes a synthesized illumination harmonization image, one object illumination and one background illumination ground-truths. A visual six-tuple example is shown in Figure 2.

3.2. Dataset analysis

To provide a deeper understanding of our dataset, we provide a series of the statistics on the ratio of real objects (*i.e.*, occluders), real-world shadows, virtual objects, and illumination, as illustrated in Figure 3. The area distribution is expressed as the ratio between the target (*i.e.*, shadows, occluders or virtual objects) area and the whole image area. We observe that the majority of occluders and virtual objects fall in $(0.1, 0.4]$ and $(0.1, 0.3]$ respectively, as shown in Figure 3 (a)-(b). The ratio of shadow area falls

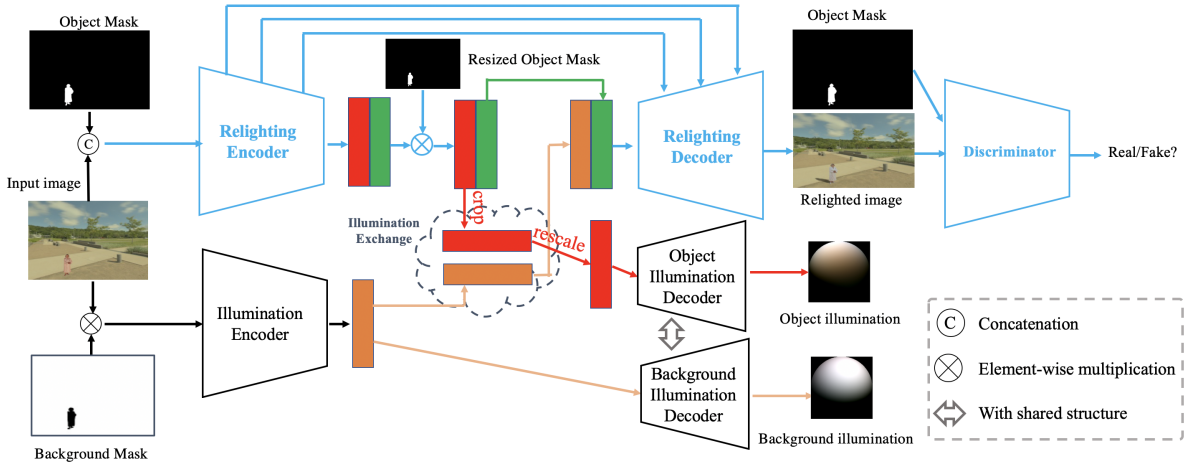

Figure 4. The overview of our proposed SI-GAN. Given an input image with inserted object and the corresponding object mask and background mask, the generator of our SI-GAN can generate the relighting image (R-Network) and predict both object illumination and background illumination (I-Network), and the discriminator can distinguish whether the generated relighting image is real or fake. The Illumination exchange mechanism between the R-Network and the I-Network realizes the conversion of illumination information between the scene and the object.

in $(0.08, 0.3]$ (see Figure 3 (c)), which illustrates that large-area non-shadow area is potentially suitable for inserting object of interest.

Also, we analyze the spatial distribution of illumination in the scene in our dataset by computing a probability map to show how likely a pixel belongs to the illumination range. Figure 3 shows that the illumination tends to cluster around the lower center of the image, since inserted objects are often placed approximately around the human eyesight.

4. Proposed Method

Our goal is to train a GAN that takes a synthesis image $\hat{Y}$ without illumination harmonization, corresponding the object mask, background mask and corresponding target illumination as input, and directly generate the corresponding scene illumination harmonized image $\bar{Y}$. To achieve this goal, we propose a novel framework called SI-GAN, of which the generator is a multi-task parallel network composed of two networks, *i.e.*, relighting network (R-Network) and Illumination network (I-Network) to handle object and illumination separately, as shown in Figure 4. In particular, R-Network is used to estimate the overall input information and achieve the synthetic image illumination harmony by using multi-scale attention mechanism and illumination exchange mechanism, and I-Network is used to estimate the background and object illumination information. Note that there is an illumination exchange component to ensure the inserted object obtain the harmonious illumination to generate a realistic synthetic image. Meanwhile, a discriminator is designed to verify whether the inserted object in the generated relighting image has consistent illumination with background.

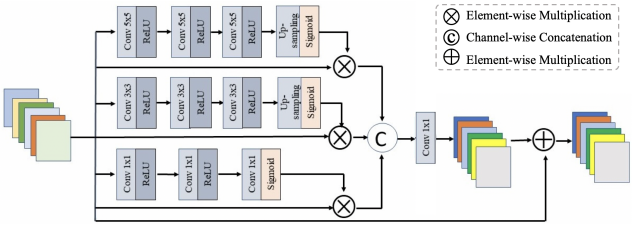

Figure 5. The structure of multi-scale attention mechanism.

4.1. Generator

As shown in Figure 4, the generator of our SI-GAN contains two parallel branch networks, *i.e.*, R-Network and I-Network. R-Network learns the overall features of the input image and I-network predicts the object and background illumination. They work collaboratively to complete the task.

Relighting Encoder. For the U-Net [28] like R-Network, there are five down-sampling blocks in encoder and each down-sampling blcok consists of a residual block with 3 consecutive convolutions, batch normalization and ReLU operation and halves the feature map with an average pooling operation. Each down-sampling block is followed by a multi-scale attention block which guides the network to infer the object shadow and generates the refinement feature maps. Note that we design such a multi-scale attention mechanism for two purposes: (1) to adaptively extract reliable multi-scale features and overcome the scale-variation across the image to assign larger weights to areas of interest for refinement purpose; and (2) to guide the generation of shadows of the inserted objects by paying attention to real shadows and correspond occluders in real-world image.

As shown in Figure 5, the multi-scale attention block has three types convolution layers with three different kernel sizes, 1×1, 3×3, 5×5, to extract features in different scales. Specially, for the input feature map, the multi-scale attention block first extracts features using two 1×1 convo-

lution layers with crossing channels and squeezing features, two 3×3 convolution layers and two 5×5 convolution layers to generate feature maps. Note that for 3×3 and 5×5 convolution, the feature map size of each channel has been changed and therefore we apply an up-sampling layer to recover the original size before feeding the feature map into the Sigmoid function to produce attention map. We conduct an element-wise multiplication on the input feature and the attention map at each scale separately to produce attended feature maps, which are then concatenated at channel-wise together and fed into a 1×1 convolution layer to recover the same channel number with the origin input feature. We apply a residual structure [9] to combine it with the origin input feature map together as final output. This residual mechanism not only accelerates the convergence speed but also correct image details such as border artifacts.

The final output features of the encoder include the illumination features F_{illu} and non-illumination features F_{noillu} of global image. This feature separation is enforced by the no-illumination loss $\mathcal{L}_{noillu}$ (see Equation 3).

Illumination Encoder. For the I-Network, the encoder structure is similar to the one of the R-Network and outputs the illumination feature of the background image.

Illumination Exchange Mechanism. After obtaining the features extracted by the two encoders, we exchange the object illumination features in the R-Network with the background illumination features in the I-Network.

To specify, these two sub-networks work together through the illumination exchange mechanism. It is worth mentioning that at the bottleneck feature of the R-Network, we performed the multiplication operation on it with the object mask of the corresponding size and get the feature F^{obj} for foreground object. This treatment is able to better realizes the exchange of object illumination and background illumination, and achieve the illumination harmonization task.

The object feature F^{obj} can be divided into two parts: synthetic image feature F^{obj}_{noillu} which is independent of illumination feature F^{obj}_{illu}. The illumination feature F^{obj}_{illu} is cropped by the resized object mask, rescaled to a larger size and then fed into the object illumination decoder of the I-Network to predict the object illumination. The background illumination feature F^{bg}_{illu} extracted by the I-Network decoder and F^{bg}_{illu} concatenated together and fed into the R-Network decoder part to generate the realistic Illumination harmony image. In the whole illumination harmony task, we have supervised constraints on the relighting image, the non-illuminated and illumination feature of the object, and the background illumination feature, respectively, which improves the harmony accuracy of the relighting image.

Relighting Decoder. The decoder in the R-Network consists of five up-sampling layers. Each up-sampling layer doubles the feature map by nearest interpolation followed by consecutive dilated convolution, batch normalization and ReLU operations. The last feature map is activated by a sigmoid function. The R-network concatenates down-up sampling layers by skip connections The final output of the R-network is the harmonized image with plausible object shadow and illumination.

Object/Background Illumination Decoders. Following [34], the decoder of the I-Network is to predict the illumination. In this paper, we use the shared structure for both object illumination and background illumination decoders.

4.2. Discriminator

The discriminator of SI-GAN is designed to help the R-network accelerate convergence and generate a plausible harmonized image. Following Patch-GAN [14], our discriminator consists of six consecutive convolutional layers. Each convolutional layer contains convolution, instance normalization and ReLU operations. We use Sigmoid function to activate last feature map produced by a convolution, and perform a global average pooling operation on the activated feature map to obtain the final output of the discriminator. The discriminator takes the concatenation of the generated relighted image and object, or the concatenation of the ground-truth relighted image and the object mask, as input to determine real or fake.

4.3. Loss functions

The total loss $\mathcal{L}_{total}$ is formulated with an illumination loss $\mathcal{L}_{illu}$, a perceptual loss $\mathcal{L}_{per}$, and an adversarial loss $\mathcal{L}_{adv}$ as follows:

$$\mathcal{L}_{total} = \beta_1 \mathcal{L}_{illu} + +\beta_2 \mathcal{L}_{noillu} + \beta_3 \mathcal{L}_{per} + \beta_4 \mathcal{L}_{adv}, \quad (1)$$

where β_1, β_2 , β_3, β_4 are hyper-parameters which control the influence of terms.

Illumination loss $\mathcal{L}_{illu}$ is the element-wise illumination loss between the generated illumination and the corresponding ground truth, *i.e.*,

$$\mathcal{L}_{illu} = \|Y_{OI} - \bar{Y}_{OI}\|_2^2 + \|Y_{BI} - \bar{Y}_{BI}\|_2^2, \quad (2)$$

where $\bar{Y}_{OI}$ and $\bar{Y}_{BI}$ represent the output virtual object illumination image, and background illumination image, respectively. Y_{FI} and Y_{BI} are their corresponding ground truth image.

Non-illumination feature loss $\mathcal{L}_{nonillu}$ is further introduced to enforce non-illumination feature matching to improve the accuracy of the object relighting image. According to the lightness and Retinex theory [20], reflectance is the inherent physical property of object, independent of illumination. Therefore, we hope that the same object under different illumination conditions have the same non-illumination (*i.e.*, reflectance) features, mathematically expressed as

$$\mathcal{L}_{nonillu} = \frac{1}{N_{nonillu}}(F^1_{nonillu} - F^2_{nonillu})^2, \quad (3)$$

where $F^1_{nonillu}$ and $F^2_{nonillu}$ are non-illumination features of a same insert object under two different illumination conditions, and $N_{nonillu}$ is the number of elements in $F_{nonillu}$.

Perceptual loss $\mathcal{L}_{per}$ [15] is used to measure the semantic difference between the generated image and the ground truth. Following [25], we use a VGG-16 model [29] pre-trained on ImageNet dataset [4] to extract feature and choose the first 10 VGG16 layers to compute feature map. $\mathcal{L}_{per}$ is defined as:

$$\begin{aligned}\mathcal{L}_{per} =& \text{MSE}(V_{Y_{FI}}, V_{\bar{Y}_{FI}}) + \text{MSE}(V_{Y_{BI}}, V_{\bar{Y}_{BI}}) \\ &+ \text{MSE}(V_{Y_R}, V_{\bar{Y}_R})\end{aligned} \quad (4)$$

where MSE is the mean squared error, and $V_i = \text{VGG}(i)$ is the extracted feature map.

Adversarial loss $\mathcal{L}_{adv}$ is utilized to describe the competition between the generator and the discriminator as:

$$\mathcal{L}_{adv} = \log(\mathbf{D}(x, m, Y)) + \log(1 - \mathbf{D}(x, m, \bar{Y})), \quad (5)$$

where $\mathbf{D}(\cdot)$ is the probability that the image is "real". x is the input image and m is the corresponding mask, $\bar{Y}$ is the output of the generator of SI-GAN, and Y is the ground-truth. The discriminator tries to maximize $\mathcal{L}_{adv}$ while the generator tries to minimize it.

4.4. Implementation details

Our SI-GAN model is implemented by Tensorflow and runs with NVIDIA GeForce GTX 1080Ti GPU. We randomly select 80% of images as the training set, and take the rest 20% images as the testing set. Our network is trained for 80 epochs with bach size 1, and the resolution of all images for training and testing is 256×256. We set decay as 0.9 for batch normalization and all the batch normalization share the same hyper parameters. The initial learning rate is 10^{-4}. We set β_1 = 25.0, β_2 = 6.0, β_3 = 0.04, β_4 = 0.5 for loss item and adopt Adam optimizer to optimize the SI-GAN and discriminator. It takes about 98 hours to complete the entire training.

5. Experiments

In this section, we evaluate our proposed SI-GAN both quantitatively and qualitatively, and compare it with state-of-the-art methods on our constructed dataset IH.

5.1. Evaluation Metrics and Experimental Settings

Evaluation metrics. We use three evaluation metrics, *i.e.*, root mean square error (RMSE), peak signal to noise ratio (PSNR) and structural similarity index (SSIM) between a generated harmonized image and the corresponding ground truth on the test set. In general, with the smaller RMSE, the larger SSIM and PSNR, the generated illumination harmonized image is better.

Table 1. Quantitative comparison results on our testing set. The best results are marked in bold.

Method	RMSE	SSIM	PSNR
ASI3D [17]	0.024	0.827	35.247
ASMOR [24]	0.013	0.914	39.64
ARShadowGAN [25]	0.008	0.928	41.512
SI-GAN	**0.005**	**0.964**	**43.107**

Compared methods. Our task is to edit the illumination of the image-based object inserted into the real-world scene image to achieve the illumination harmony between them for augmented reality. To our best knowledge, there are only a few traditional methods conducting the similar tasks and no existing deep learning-based method. In this paper, we choose two traditional methods similar to our task, *i.e.*, ASI3D [17] and ASMOR [24], and a deep learning-based method ARShadowGAN [25] which we extend for our task to compare with. For ASI3D and ASMOR, to ensure their relighting systems can generate harmonized image directly, we strictly follow their input requirements and feed them with the corresponding inputs. For ARShadowGAN method [25], we also use the same input as our SI-GAN for fair comparison.

5.2. Comparison with Start-of-the-art Methods

We analyze the performance of our SI-GAN and state-of-the-art methods for object illumination editing as follows:

Quantitative comparison. Table 1 reports the quantitative comparison results on our testing set. As can be seen, (1) although ASI3D and ASMOR are traditional methods, ASMOR's performance in terms of three evaluation metrics is close to that of ARShadowGAN; (2) ARShadowGAN is slightly better than ASMOR, but obviously outperforms ASI3D; and (3) our SI-GAN achieves the best quantitative results on all these three evaluation metrics.

This is mainly because the traditional methods ASI3D and ASMOR rely on the estimation accuracy of 3D information of objects and scenes. With no doubts, inaccurate estimation of 3D information often leads to poor results. As a deep learning based method, our SI-GAN does not require complicated 3D information estimation and instead it uses the attention mechanism to enhance the beneficial features for a better result. The best performance of SI-GAN is mainly attributed to the multi-scale attention mechanism, feature exchange mechanism and adversarial learning, which can better guide the illumination editing of inserted object, refine the features and bridge the illumination gap between inserted object and background environment to obtain results closer to the ground truth.

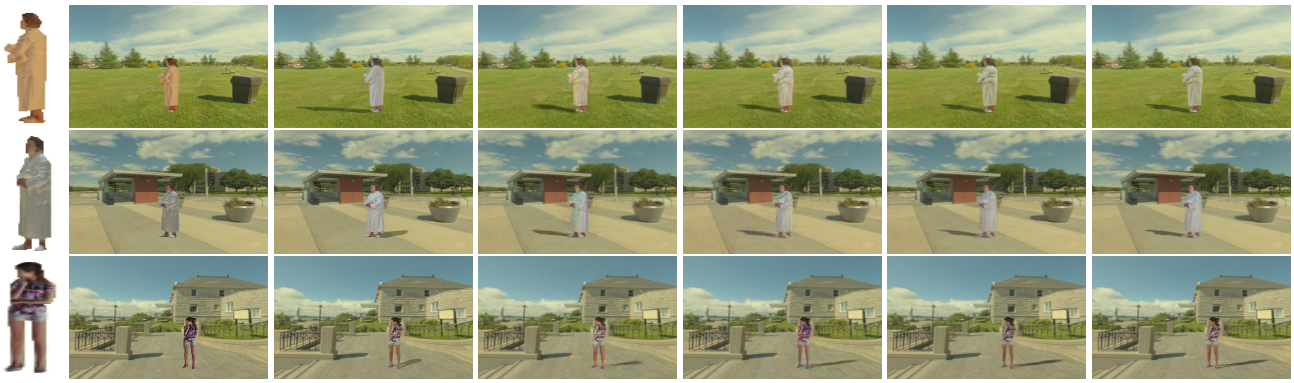

(a) (b) (c) (d) (e) (f) (g)

Figure 6. Visual comparison of our method against other start-of-the-art methods on the testing set of our dataset. From left to right are: (a) 3D object, (b) input image, the results of (c) ASI3D, (d) ASMOR, (e) ARShadowGAN and (f) SI-GAN, (g) ground truth.

Visual comparison. To compare the performance of the methods more intuitively, we provide some visual comparison results in Figure 6. As we can see, our SI-GAN not only achieves the illumination transformation of different scenes, but also gains the best visual results with plausible object shadows and harmonious illumination.

Among these competing methods, ASID3D and ASMOR estimate the inaccurate or wrong information of geometry and illumination of the object and scene. Although ARShadowGAN generates reasonable object shadows, it has weak illumination processing and therefore cannot reasonably edit the object illumination information.

In contrast, SI-GAN is able to achieve the better results with plausible object shadow and harmonious illumination, which mainly because our network makes full use of the collaborative R-Network and I-Network parallel with the multi-scale attention mechanism, the illumination feature exchange mechanism, and the adversarial learning strategy to automatically infer the shadow and illumination generation of the object. Our proposed multi-scale attention mechanism plays a role in inferring scene and refining features. Moreover, our feature exchange mechanism is able to greatly achieve illumination features exchange between the object and corresponding background for illumination harmonization. Our SI-GAN avoids the complicated inverse rendering process and directly generates reasonable illumination harmonized results.

5.3. Ablation Study

We conduct ablation study to investigate the effectiveness of each main component of our loss function and network architecture respectively. To this end, we perform experiments to evaluate the performance of the proposed multi-scale attention mechanism (MSA), illumination exchange mechanism (IEM) and perceptual loss $\mathcal{L}_{per}$, non-illumination feature loss $\mathcal{L}_{nonillu}$ and adversarial loss $\mathcal{L}_{adv}$.

The quantitative and visual comparison results are shown in Table 2 and Figure 7, respectively. As we can see in Table 2, our SI-GAN with all components is able to obtain better results than other methods with one or two components in all three evaluation metrics. By comparing SI-GAN with "Basic + MSA + $\mathcal{L}_{nonillu}$ + $\mathcal{L}_{adv}$ + IEM", "Basic + MSA + $\mathcal{L}_{per}$ + $\mathcal{L}_{nonillu}$ + IEM" and "Basic + $\mathcal{L}_{per}$ + $\mathcal{L}_{nonillu}$ + $\mathcal{L}_{adv}$ + IEM" respectively in Table 2, we find that our proposed multi-scale attention mechanism and the used perceptual loss ($\mathcal{L}_{per}$) and adversial loss ($\mathcal{L}_{adv}$) are all beneficial to our final results.

Table 2. Ablation study. "Basic" denotes our method without multi-scale attention mechanism (MSA), IEM and the used perceptual loss $\mathcal{L}_{per}$, non-illumination feature loss $\mathcal{L}_{nonillu}$, and adversarial loss $\mathcal{L}_{adv}$. The best results are marked in bold.

Method	RMSE	SSIM	PSNR
Basic	0.0174	0.927	37.824
Basic + MSA + IEM	0.0069	0.950	40.024
Basic + $\mathcal{L}_{adv}$ + IEM	0.0098	0.946	39.982
Basic + $\mathcal{L}_{per}$ + IEM	0.0123	0.937	38.356
Basic + $\mathcal{L}_{per}$ + $\mathcal{L}_{nonillu}$ + $\mathcal{L}_{adv}$ + IEM	0.0072	0.950	41.204
Basic + MSA + $\mathcal{L}_{adv}$ + $\mathcal{L}_{nonillu}$ + IEM	0.0057	0.968	43.316
Basic + MSA + $\mathcal{L}_{per}$ + $\mathcal{L}_{nonillu}$ + IEM	0.0064	0.953	41.336
Basic + MSA + $\mathcal{L}_{adv}$ + $\mathcal{L}_{per}$ + IEM	0.0053	0.973	43.407
Basic + MSA + $\mathcal{L}_{per}$ + $\mathcal{L}_{nonillu}$ + $\mathcal{L}_{adv}$	0.0069	0.950	40.925
SI-GAN	**0.0051**	**0.976**	**44.463**

From Figure 7 we observe that SI-GAN generates better object shadow and illumination than "Basic + MSA + IEM + $\mathcal{L}_{per}$ + $\mathcal{L}_{nonillu}$" with odd-looking object shadow and illumination. The "Basic + MSA + IEM + $\mathcal{L}_{per}$ + $\mathcal{L}_{nonillu}$" yields this worse results mainly because the network has not converged, which highlights the advantage of adversarial learning to accelerate network convergence in the task. Another observation is that "Basic + IEM + $\mathcal{L}_{per}$ + $\mathcal{L}_{nonillu}$ + $\mathcal{L}_{adv}$" produces a relatively poor result with coarse object shadow and unnatural illumination compared to SI-GAN, which demonstrates that our proposed multi-scale attention mechanism can make full use of important features to guide the shadow generation of inserted object and refine the extracted useful features of different scales. In addition, we find that the object obtained a poor illumination result from (f), mainly because there is no IEM to exchange illumination information. Although result (g) is closer to the best

(a) (b) (c) (d) (e) (f) (g) (h) (i)

Figure 7. Ablation study for our SI-GAN. (a) Input image without illumination harmonization. (b) mask. (c) Basic + MSA + IEM + $\mathcal{L}_{per}$ + $\mathcal{L}_{nonillu}$. (d) Basic + IEM + $\mathcal{L}_{per}$ + $\mathcal{L}_{nonillu}$ + $\mathcal{L}_{adv}$. (e) Basic + MSA + IEM + $\mathcal{L}_{nonillu}$ + $\mathcal{L}_{adv}$. (f) Basic + MSA + $\mathcal{L}_{per}$ + $\mathcal{L}_{nonillu}$ + $\mathcal{L}_{adv}$. (g) Basic + MSA + IEM + $\mathcal{L}_{adv}$ + $\mathcal{L}_{per}$. (h) SI-GAN. (i) Ground truth. *Please zoom in to observe the detailed difference.*

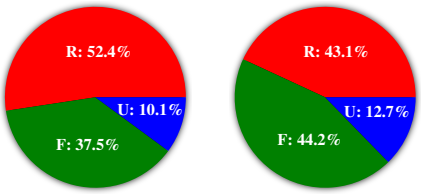

(a) Real images (b) Synthesis images

Figure 8. Perceptual study results on real and synthesis images. "R" and "F" indicate the visually realistic and fake relighting results respectively, while "U" indicates that the result is uncertain whether users result in an agreement.

one produced by our SI-GAN, the appearance of the object of SI-GAN is more refined,

which indicates that the non-illumination feature loss $\mathcal{L}_{nonillu}$ can promote our network to generate a more accurate illumination harmony image.

5.4. Perceptual User Study

To further evaluate the quality of illumination harmonization images produced by our SI-GAN. We follow the method [22] to conduct a simple perceptual study. We select the total of 100 images with different illumination. Fifty images with illumination harmonization are from the real-world and the others are generated by our SI-GAN. The resolution of all images is set to 512×512.

Then we recruited 100 participants from a school campus, including professional image processing researchers, 3D-Max and Photoshop users, and senior art scholars. We divide each image into three visual levels: (1) *Real*: realistic and harmonious illumination image, (2) *Fake*: unrealistic illumination image with artifacts, (3) *Uncertain*: uncertain image which they can't make a decision, and ask them to give their judgment results. The results of user study is shown in Figure 8. As we can see, 52.4% of real images are judged to be real images and the other real images are judged to be fake image or uncertain image. At the same time, 43.1% of the synthesis images from our SI-GAN are judged to be real image, which has almost the same judgment result as the real images. This fully proves that our network has good performance in processing illumination harmonization task.

5.5. Discussions

Generalization. To verify the generalization of our method, we also test our SI-GAN on 200 real-world images in the illumination controllable indoor environment. We also adopt the same perceptual user study as done in Section 5.4 to evaluate all results produced by our method on the 200 testing images. Subjects agree that 62.1%, 21.3% and 16.6% of all results are real, fake and uncertain, which illustrates that SI-GAN has a strong generalization ability on real-world images.

Limitations. Our SI-GAN has two limitations. Firstly, SI-GAN generally works better in outdoor scenes than indoor scenes, since indoor scenes are sometimes with relatively dark lighting. Secondly, SI-GAN may fail to edit the object illumination under multiple light sources. We left this as our future work.

6. Conclusion and Feature Work

In this work, we have presented a large-scale and high-quality dataset IH and proposed a novel deep learning-based method SI-GAN to edit the image-based object illumination and generate visually plausible illumination harmonized result without any intermediate inverse rendering process. In the future, we will extend our SI-GAN to be used for object illumination editing under multiple light sources, and handle video illumination harmony.

References

[1] Martin Arjovsky, Soumith Chintala, and Léon Bottou. Wasserstein gan. In *International conference on Machine Learning*, 2017. 2

[2] Jonathan T Barron and Jitendra Malik. Intrinsic scene properties from a single rgb-d image. *IEEE Computer Society Conference on Computer Vision and Pattern Recognition*, 38(4), 2013. 2

[3] Wenyan Cong, Jianfu Zhang, Li Niu, Liu Liu, and Liqing Zhang. Dovenet: Deep image harmonization via domain verification. In *the IEEE Conference on Computer Vision and Pattern Recognition*, 2020. 2, 3

[4] Jia Deng, Wei Dong, Richard Socher, Li Jia Li, and Fei Fei Li. Imagenet: A large-scale hierarchical image database. In *Proceedings of the IEEE Conference on Computer Vision and Pattern Recognition*, 2009. 6

[5] Bin Ding, Chengjiang Long, Ling Zhang, and Chunxia Xiao. Argan: Attentive recurrent generative adversarial network for shadow detection and removal. In *Proceedings of the IEEE International Conference on Computer Vision*, 2020. 2

[6] Marc-André Gardner, Yannick Hold-Geoffroy, Kalyan Sunkavalli, Christian Gagné, and Jean-François Lalonde. Deep parametric indoor lighting estimation. In *Proceedings of the IEEE International Conference on Computer Vision*, pages 7175–7183, 2019. 2, 3

[7] Marc-André Gardner, Kalyan Sunkavalli, Ersin Yumer, Xiaohui Shen, Emiliano Gambaretto, Christian Gagné, and Jean-François Lalonde. Learning to predict indoor illumination from a single image. *ACM Transactions on Graphics*, 36(6), 2017. 2, 3

[8] Ian Goodfellow, Jean Pouget-Abadie, Mehdi Mirza, Bing Xu, David Warde-Farley, Sherjil Ozair, Aaron Courville, and Yoshua Bengio. Generative adversarial nets. In *Advances in neural information processing systems*, pages 2672–2680, 2014. 2

[9] Kaiming He, Xiangyu Zhang, Shaoqing Ren, and Jian Sun. Deep residual learning for image recognition. In *Proceedings of the IEEE conference on computer vision and pattern recognition*, 2016. 5

[10] Tao Hu, Chengjiang Long, and Chunxia Xiao. A novel visual representation on text using diverse conditional gan for visual recognition. *IEEE Transactions on Image Processing*, 30:3499–3512, 2021. 2

[11] Xiaowei Hu, Yitong Jiang, Chi Wing Fu, and Pheng Ann Heng. Mask-shadowgan: Learning to remove shadows from unpaired data. In *Proceedings of the IEEE International Conference on Computer Vision*, 2019. 2

[12] Ashraful Islam, Chengjiang Long, Arslan Basharat, and Anthony Hoogs. Doa-gan: Dual-order attentive generative adversarial network for image copy-move forgery detection and localization. In *Proceedings of the IEEE Conference on Computer Vision and Pattern Recognition*, 2020. 2

[13] Ashraful Islam, Chengjiang Long, and Richard Radke. A hybrid attention mechanism for weakly-supervised temporal action localization. In *AAAI Conference on Artificial Intelligence (AAAI)*, 2021. 2

[14] Phillip Isola, Jun-Yan Zhu, Tinghui Zhou, and Alexei A Efros. Image-to-image translation with conditional adversarial networks. In *Proceedings of the IEEE Conference on Computer Vision and Pattern Recognition*, pages 1125–1134, 2017. 3, 5

[15] Justin Johnson, Alexandre Alahi, and Li Fei-Fei. Perceptual losses for real-time style transfer and super-resolution. In *European Conference on Computer Vision*, 2016. 6

[16] Kevin Karsch, Varsha Hedau, David Forsyth, and Derek Hoiem. Rendering synthetic objects into legacy photographs. page 1, 2011. 2

[17] Kevin Karsch, Kalyan Sunkavalli, Sunil Hadap, Nathan Carr, Hailin Jin, Rafael Fonte, Michael Sittig, and David Forsyth. Automatic scene inference for 3d object compositing. *ACM Transactions on Graphics*, 33(3):1–15, 2014. 1, 2, 6

[18] Jiwon Kim, Jung Kwon Lee, and Kyoung Mu Lee. Accurate image super-resolution using very deep convolutional networks. In *Proceedings of the IEEE Conference on Computer Vision and Pattern Recognition*, 2016. 3

[19] Jean-François Lalonde, Derek Hoiem, Alexei A Efros, Carsten Rother, John Winn, and Antonio Criminisi. Photo clip art. *ACM Transactions on Graphics*, 2007. 2

[20] Edwin H Land and John J McCann. Lightness and retinex theory. *Journal of the Optical Society of America*, 61(1):1–11, 1971. 5

[21] Christian Ledig, Lucas Theis, Ferenc Huszar, Jose Caballero, Andrew Cunningham, Alejandro Acosta, Andrew Aitken, Alykhan Tejani, Johannes Totz, Zehan Wang, et al. Photo-realistic single image super-resolution using a generative adversarial network. In *Proceedings of the IEEE conference on computer vision and pattern recognition*, 2017. 3

[22] Chen Li, Kun Zhou, Hsiang Tao Wu, and Stephen Lin. Physically-based simulation of cosmetics via intrinsic image decomposition with facial priors. *IEEE Transactions on Pattern Analysis and Machine Intelligence*, 41(6):1455–1469, 2018. 8

[23] Zicheng Liao, Kevin Karsch, and David Forsyth. An approximate shading model for object relighting. In *Proceedings of the IEEE conference on Computer Vision and Pattern Recognition*, 2015. 1, 2

[24] Zicheng Liao, Kevin Karsch, Hongyi Zhang, and David Forsyth. An approximate shading model with detail decomposition for object relighting. *International Journal of Computer Vision*, 2018. 1, 2, 6

[25] Daquan Liu, Chengjiang Long, Hongpan Zhang, Hanning Yu, and Chunxia Xiao. Arshadowgan: Shadow generative adversarial network for augmented reality in single light scenes. In *Proceedings of the IEEE Conference on Computer Vision and Pattern Recognition*, 2020. 2, 6

[26] Xiaojiao Mao, Chunhua Shen, and Yu-Bin Yang. Image restoration using very deep convolutional encoder-decoder networks with symmetric skip connections. In *Advances in neural information processing systems*, pages 2802–2810, 2016. 3

[27] Mehdi Mirza and Simon Osindero. Conditional generative adversarial nets. *Computer ence*, pages 2672–2680, 2014. 2

[28] Olaf Ronneberger, Philipp Fischer, and Thomas Brox. U-net: Convolutional networks for biomedical image segmentation. In *International Conference on Medical image computing and computer-assisted intervention*, pages 234–241. Springer, 2015. 4

[29] Karen Simonyan and Andrew Zisserman. Very deep convolutional networks for large-scale image recognition. In *International Conference on Learning Representations*. 6

[30] Bhavan Vasu and Chengjiang Long. Iterative and adaptive sampling with spatial attention for black-box model explanations. In *The IEEE Winter Conference on Applications of Computer Vision (WACV)*, March 2020. 2

[31] Jifeng Wang, Xiang Li, Le Hui, and Jian Yang. Stacked conditional generative adversarial networks for jointly learning shadow detection and shadow removal. 2017. 2

[32] Jinjiang Wei, Chengjiang Long, Hua Zou, and Chunxia Xiao. Shadow inpainting and removal using generative adversarial networks with slice convolutions. *Computer Graphics Forum*, 38(7):381–392, 2019. 2

[33] Li Xu, Jimmy SJ. Ren, Ce. Liu, and Jiaya Jia. Deep convolutional neural network for image deconvolution. *Advances in neural information processing systems*, 2:1790–1798, 2014. 3

[34] Ye Yu and William AP Smith. Inverserendernet: Learning single image inverse rendering. In *Proceedings of the IEEE Conference on Computer Vision and Pattern Recognition*, pages 3155–3164, 2019. 5

[35] Jiqing Zhang, Chengjiang Long, Yuxin Wang, Haiyin Piao, Haiyang Mei, Xin Yang, and Baocai Yin Yin. A two-stage attentive network for single image super resolution. *IEEE Transactions on Circuits and Systems for Video Technology (T-CSVT)*, 2021. 2

[36] Jiqing Zhang, Chengjiang Long, Yuxin Wang, Xin Yang, Haiyang Mei, and Baocai Yin. Multi-context and enhanced reconstruction network for single image super resolution. In *2020 IEEE International Conference on Multimedia and Expo (ICME)*, pages 1–6. IEEE, 2020. 2

[37] Ling Zhang, Chengjiang Long, Qingan Yan, Xiaolong Zhang, and Chunxia Xiao. Cla-gan: A context and lightness aware generative adversarial network for shadow removal. *Computer Graphics Forum (CGF)*, 39(7), 2020. 2

[38] Ling Zhang, Chengjiang Long, Xiaolong Zhang, and Chunxia Xiao. Ris-gan: Explore residual and illumination with generative adversarial networks for shadow removal. In *Proceedings of the AAAI Conference on Artificial Intelligence*, 2019. 2

[39] Shuyang Zhang, Runze Liang, and Miao Wang. Shadowgan: Shadow synthesis for virtual objects with conditional adversarial networks. *Computing Visual Media*, 5(1):105–115, 2019. 2

[40] Xizhou Zhu, Dazhi Cheng, Zheng Zhang, Stephen Lin, and Jifeng Dai. An empirical study of spatial attention mechanisms in deep networks. In *Proceedings of the IEEE International Conference on Computer Vision*, 2020. 2